Proceedings, Bicycle and Motorcycle Dynamics 2010
Symposium on the Dynamics and Control of Single Track Vehicles,
20–22 October 2010, Delft, The Netherlands

Rider control of a motorcycle near to its cornering limits

R. S. Sharp*

* Department of Mechanical, Medical and Aerospace Engineering
Faculty of Engineering and Physical Sciences
University of Surrey
Guildford GU2 7XH, UK
e-mail: robinsharp@waitrose.com

ABSTRACT

Optimal linear quadratic control theory is applied to longitudinal and lateral control of a high-performance motorcycle. Central to the story is the use of sufficient preview of the road to obtain the full benefit available from it. The focus is on effective control near to the cornering limits of the machine and gain scheduling according to speed and lateral acceleration is employed to ensure that the linear controller used at any time is that most appropriate to the running conditions.

The motorcycle model employed and the control theory background are described briefly. Optimal preview controls and closed-loop system frequency responses are illustrated. Path-tracking simulations are discussed and results are shown. Excellent machine control near to the feasible cornering limit is demonstrated.

Keywords: motorcycle, rider, optimal preview control, limit, adaptation, gain scheduling, frequency response, path tracking.

1 INTRODUCTION

An optimal-preview-control-based theory for high-quality car driving and motorcycle, bicycle and unicycle riding has been under development for several years [1, 2, 3, 4, 5, 6, 7, 8, 9, 10, 11, 12]. The theory relies on the following ideas: (i) skilled piloting (used to describe vehicle control generally) is a low-bandwidth, smooth activity, which becomes optimal control in the limit; (ii) the necessary control depends heavily on adequate path preview - the pilot needs to know the intended path or to be able to see it clearly for some distance ahead; (iii) the control also depends on the pilot knowing the dynamics of the vehicle; (iv) linear optimal preview control theory can be used to find the control inputs, to steering, throttle and brake, which minimize path-tracking errors, while conserving control power, for operating regimes describable by linear, constant-coefficient equations; (v) the full range of operation of a well-engineered vehicle can be split into such regimes by finding dynamic equilibrium (trim) states and considering small perturbations from such states; (vi) this implies that locally optimal controls can be found. Such controls can be installed as they become appropriate, according to the running state of the vehicle.

Once the method had been established for near-straight-running [1], steering control of a simple car with saturating tyre lateral forces was studied, first in front-axle-limited form [10] and then in rear-axle-limited form [11]. Scheduling by front-axle sideslip and by rear-axle sideslip respectively were shown to yield excellent control in near-limit cornering. The technique was applied to speed control [5, 8] and then to combined longitudinal and lateral controls such that tracking of paths defined by both x- and y-displacements at regular time intervals became feasible [13, 14]. The

procedure requires that a nonlinear simulation model of a specified vehicle is run to steady state to establish a whole spectrum of trim conditions; that a small-perturbation, linear model uses each trim state to establish a locally-valid linear model; that each linear model is used to generate a locally-optimal control; and these controls are used in the gain-scheduling scheme which ensures controls appropriate to the running conditions in a general manoeuvre.

In the present case, the previously separate representations of steering and speed control for a high-fidelity and well-documented motorcycle [15, 16] are combined into simultaneous path and speed (x, y, t) controls. Optimal throttle, steering and rider-lean controls are generated for trim states with variations in speed and lateral acceleration, and they are used to illustrate how the controls change as the running conditions alter. The properties of the rider-controlled motorcycle are illustrated by frequency response calculations. Path-tracking simulations, with gain-scheduling to follow variations in speed and lateral acceleration, are used to verify that the controls are capable of good operation near to cornering limits.

2 CONTROL THEORY BACKGROUND

The nonlinear continuous-time motorcycle model is linearized for operation in the vicinity of a defined trim state. The linear model resulting will normally have constant coefficients. The model is arranged to include the absolute longitudinal and lateral displacements of its reference point as states and to have normalized throttle displacement, steering torque and rider-upper-body lean torque as control inputs. The linear model is put into discrete-time form, using a time step of Ts, chosen to accommodate the highest-frequency modes included. In an inertial reference system, a path longitudinal and lateral profile is defined by discrete (x, y) points which are Ts apart in time. In the inertial reference system, illustrated in Figure 1, the road dynamics are those of a shift register or delay line and the equations describing these dynamics are of the same form as the equations of the vehicle. The two sets of equations are combined to yield a composite system, with its state-vector having a partition for the motorcycle and a partition for the road. At this first stage, the motorcycle part and the road part are uncoupled.

Suppose the discrete-time linearised vehicle equations are:

$$\boldsymbol{x_v}(k+1) = \mathbf{A_v}\boldsymbol{x_v}(k) + \mathbf{B_v}\boldsymbol{\tau}(k) \tag{1}$$

$$\boldsymbol{y_v}(k) = \mathbf{C_v}\boldsymbol{x_v}(k) \tag{2}$$

with discrete-time counter k, vehicle state vector $\boldsymbol{x_v}$ and control input $\boldsymbol{\tau}$, and let the road equation be:

$$\boldsymbol{\eta_r}(k+1) = \mathbf{A_r}\boldsymbol{\eta_r}(k) + \mathbf{B_r}\boldsymbol{\eta_{rn}}(k) \tag{3}$$

with $2n_p$ x 1 road state $\boldsymbol{\eta_r}$ and road sample values that enter the system at time kTs being the 2 x 1 $\boldsymbol{\eta_{rn}}$, 2 being the number of previewable disturbances and n_p being the number of preview steps included. In the present case, the input is:

$$\boldsymbol{\tau}(k) = [g_1 \;\; \tau_s \;\; \tau_r]^T \tag{4}$$

g_1 being throttle displacement, τ_s being steer torque and τ_r being rider-upper-body lean torque. $\boldsymbol{\eta_{rn}}$ here represents both x-displacement and y-displacement demands.

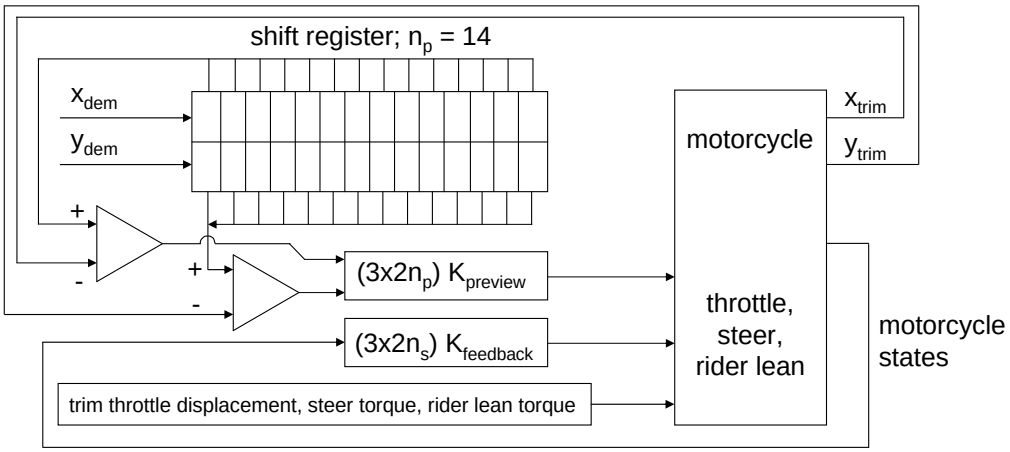

Figure 1. Diagrammatic representation of a motorcycle tracking a specified path, with the whole system referenced to ground. Such a description implies that the road sample values pass through a serial-in, parallel-out shift register operation at each time step. x_{dem} and y_{dem} define the intended path while x_{trim} and y_{trim} are the discrete path points at intervals Ts implied by the current trim state. Control inputs are sums of trim controls, state-feedback and path-preview contributions.

To represent the road shift register process, $\mathbf{A_r}$ is $2n_p$ x $2n_p$ and has the form:

$$\mathbf{A_r} = \begin{bmatrix} \mathbf{0_2} & \mathbf{I_2} & \mathbf{0_2} & \dots & \mathbf{0_2} \\ \mathbf{0_2} & \mathbf{0_2} & \mathbf{I_2} & \dots & \mathbf{0_2} \\ \vdots & \vdots & \vdots & \ddots & \vdots \\ \mathbf{0_2} & \mathbf{0_2} & \mathbf{0_2} & \dots & \mathbf{I_2} \\ \mathbf{0_2} & \mathbf{0_2} & \mathbf{0_2} & \dots & \mathbf{0_2} \end{bmatrix} \tag{5}$$

and $\mathbf{B_r}$, corresponding to the two previewable disturbances, is $2n_p$ x 2 and has the form:

$$\mathbf{B_r} = \begin{bmatrix} 0 & 0 & 0 & 0 & 0 & 0 & \dots & 1 & 0 \\ 0 & 0 & 0 & 0 & 0 & 0 & \dots & 0 & 1 \end{bmatrix}^T \tag{6}$$

Here, $\mathbf{0_2}$ is a 2 x 2 zero matrix while $\mathbf{I_2}$ is a 2 x 2 identity matrix.

Combining vehicle and road equations together, the full dynamic system is defined by:

$$\begin{bmatrix} \boldsymbol{x_v}(k+1) \\ \boldsymbol{\eta_r}(k+1) \end{bmatrix} = \begin{bmatrix} \mathbf{A_v} & 0 \\ 0 & \mathbf{A_r} \end{bmatrix} \begin{bmatrix} \boldsymbol{x_v}(k) \\ \boldsymbol{\eta_r}(k) \end{bmatrix} + \begin{bmatrix} \mathbf{B_v} \\ 0 \end{bmatrix} \boldsymbol{\tau}(k) + \begin{bmatrix} 0 \\ \mathbf{B_r} \end{bmatrix} \boldsymbol{\eta_{rn}}(k) \tag{7}$$

which takes the standard discrete-time form:

$$\boldsymbol{z}(k+1) = \mathbf{A}z(k) + \mathbf{B}\boldsymbol{u}(k) + \mathbf{E}\boldsymbol{\eta_{rn}}(k) \tag{8}$$

$$\boldsymbol{y}(k) = \mathbf{C}\boldsymbol{z}(k) \tag{9}$$

If $\boldsymbol{\eta_{rn}}$ contains samples from two uncorrelated white-noise random sequences, the time-invariant optimal control which minimizes a quadratic cost function J, given that the pair $(\mathbf{A}, \mathbf{B})$ is stabilizable and that the pair $(\mathbf{A}, \mathbf{C})$ is detectable [17], is:

$$\boldsymbol{u}^*(k) = \boldsymbol{K}\boldsymbol{z}(k) \tag{10}$$

where $\boldsymbol{K} = \left(\mathbf{R} + \mathbf{B^T P B}\right)^{-1} \mathbf{B^T P A}$, given that the cost function J is:

$$J = \lim_{n\to\infty} \sum_{k=0}^{n} \{\boldsymbol{z}^{\boldsymbol{T}}(k)\mathbf{Q}\boldsymbol{z}(k) + \boldsymbol{u}^{\boldsymbol{T}}(k)\mathbf{R}\boldsymbol{u}(k)\} \tag{11}$$

and $\mathbf{P}$ satisfies the matrix-difference-Riccati equation:

$$\mathbf{P} = \mathbf{A^T P A} - \mathbf{A^T P B}\left(\mathbf{R} + \mathbf{B^T P B}\right)^{-1} \mathbf{B^T P A} + \mathbf{Q} \tag{12}$$

Here $\mathbf{Q} = \mathbf{C^T q C}$ and $\mathbf{q}$ is a diagonal weighting matrix, diag(q_1, q_2, ...), with terms corresponding to the number of performance aspects contributing to the cost function, and $\mathbf{R}$ is a 3 x 3 diagonal weighting on the control inputs, normalized throttle pedal displacement, steering torque and rider-lean torque. $\mathbf{C}$ is chosen such that the quadratic term $\boldsymbol{z}^{\boldsymbol{T}}(k)\mathbf{Q}\boldsymbol{z}(k)$ in the cost function J penalizes the sum of the squares of the differences between the (x, y) coordinates of the car's reference point and the corresponding (x, y) of the road, over the optimization horizon. Since there are only these two aspects of performance in the cost, $\mathbf{q}$ is 2 x 2.

Optimal controls are calculated using Hazell's MATLAB Toolbox [18]. The Toolbox requires only the setting up of the standard state-space (A, B, C, D) matrices, the setting of weights on tracking errors and control efforts, and the calling of special functions, for the optimal controls to be revealed. An illustration of path tracking is given in Figure 2, where the motion is referred to the motorcycle rather than the road. The transformation is explained in [1, 2, 3, 4, 6]. The preview gains inevitably fall to zero as the preview distance increases, so that the number of preview points included can be chosen, by trials, so that effectively the full benefit available is obtained. This is referred to as "full" preview. Only full preview control is of interest here, since the control quality is inevitably reduced if the preview is curtailed [19, 20].

3 MOTORCYCLE REPRESENTATION

The motorcycle model used is of high fidelity, describing a Suzuki GSX-R1000 machine. The base model with all of its parameter values is documented in [15]. The chain-drive treatment is discussed in [16]. Since those descriptions were written, the model has been re-cast so that it uses ISO-standard axes and an engine and partial transmission model has been added, so that the three control inputs to the motorcycle are normalised throttle displacement, steering torque and rider upper-body lean torque. The motorcycle geometry is shown in Figure 3 and the body structure and freedoms allowed are shown in Figure 4. The driving torque applied to the sprocket, τ_e, is restricted to positive values corresponding to positive throttle displacements. It is a function of the normalised throttle displacement, the engine speed and the motorcycle speed according to the relations:

$$f_1 = \sin\left(\arctan\left(B_t g_1 - E_t\left(B_t g_1 - \arctan\left(B_t g_1\right)\right)\right)\right)$$

$$f_2 = f_1 D_s \sin\left[C_s \arctan\left(B_s\omega - E_s\left(B_s\omega - \arctan\left(B_s\omega\right)\right)\right)\right]/\omega - f_{tq}$$

$$f_3 = 3 - 2\sin\left(\arctan\left(0.2\left(V - 15\right)\right)\right)$$

$$\tau_e = max\left(0, f_2 f_3\right)$$

with coefficients B_t = 1.8, E_t = -12, B_s = 0.0014, C_s = 1.6, D_s = 1.2e5, E_s = -8, and f_{tq} = 20, ω being the sprocket angular velocity in rad/s and V being the motorcycle speed in m/s. f_{tq} is a friction torque. The sprocket driving torque is depicted in Figure 5. The upper part of the figure

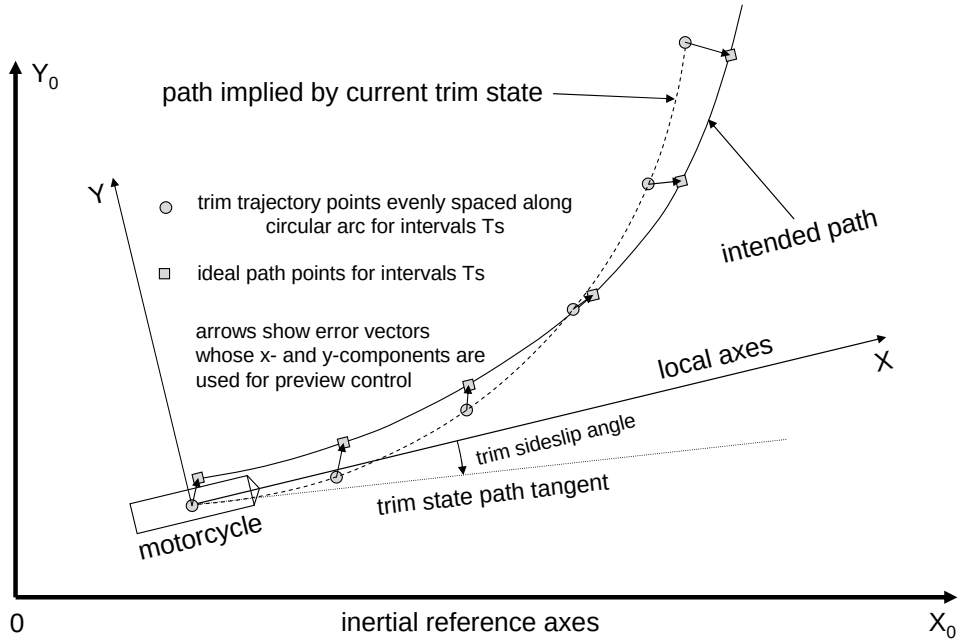

Figure 2. Snapshot of motorcycle in a general motion state using local reference axes [1, 2, 3, 4, 6]. The current trim defines points along a circular path while the intended path points are known through the preview. Differences constitute errors which are employed, together with the optimal preview gains, in the preview part of the control. Each complete control signal is made up of a trim-state part, a state-feedback part and a preview part.

shows the function f_2, with the lower part showing the gear ratio or torque multiplier function f_3. When the throttle displacement is negative, braking torques are applied in proportion to the displacement. The front brake torque acts between the lower forks and the front wheel, while that at the rear acts on the rear wheel and reacts on the swing arm. The torque ratio is set by parameters to 87.5% front, 12.5% rear.

4 CALCULATIONS

4.1 Determining trim states and optimal gains

Firstly, the nonlinear simulation model is run up slowly through its speed range in a straight line to find an approximate throttle-opening / trim-speed relationship. The approximate trim states are then used to generate rough optimal control sets for chosen speeds covering the range. These rough controls allow the motorcycle to be run under rider-control with sufficient quality to accurately track straight paths at speeds of 10, 20, 30, 40, 50, 60 and 70 m/s, establishing true trim states that can be stored. The generation of optimal controls requires that the sampling interval, Ts, and the weightings on control power and on x- and y-tracking errors to be specified. Here $\mathbf{R}$ is chosen to be diag(1000, 1, 1), reflecting the different operating ranges of the throttle displacement, the steering torque and the rider upper-body lean torque. Then, based on previous results [3, 6, 7], Ts is set to 0.05 s and a preview horizon of 10 s is chosen as representative of real riding. By trials, full preview within the 10 s horizon (200 preview points) is found to occur with $\mathbf{q}$ = diag(100, 100), which attaches equal weight to x- and y-errors.

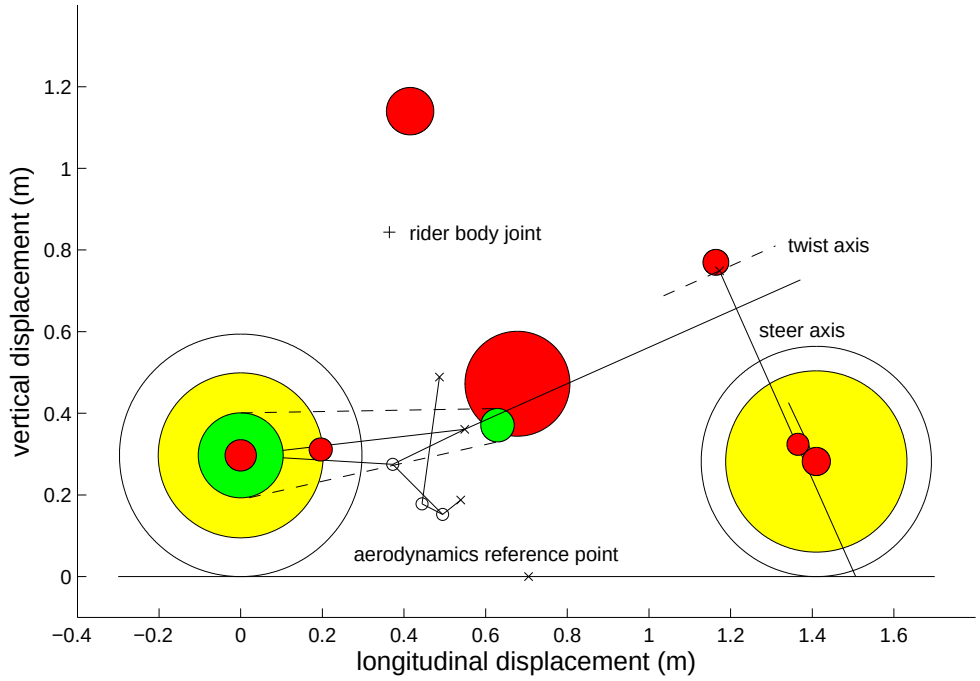

Figure 3. Scaled motorcycle model showing the masses of the seven rigid bodies included, each with area in proportion to mass.

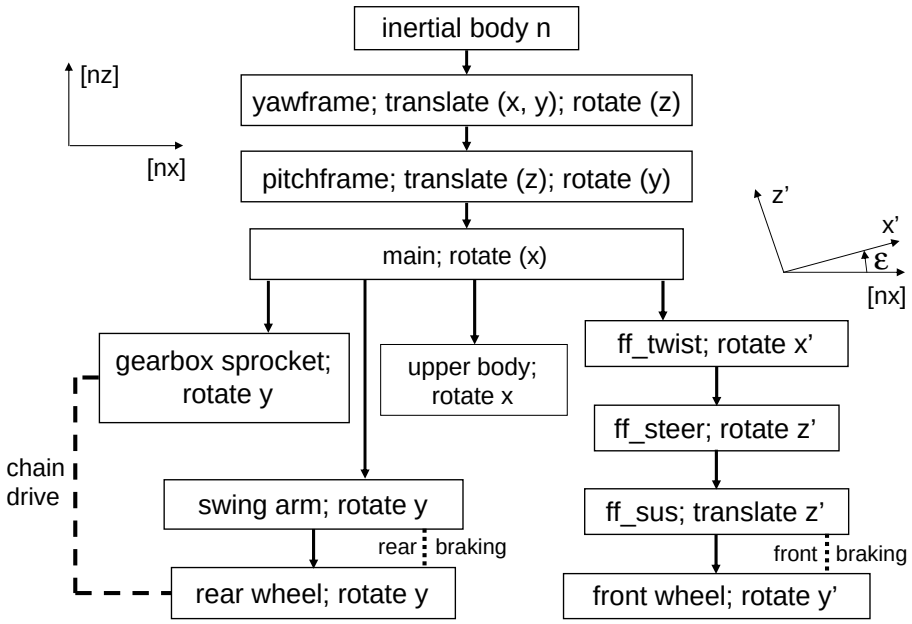

Figure 4. Motorcycle model bodies showing tree structure and freedoms allowed.

Accurate optimal controls can now be obtained from the stored straight-running trim states, so that a clothoid path, having curvature increasing in proportion to distance travelled [21], can be followed at a chosen speed of say $10\,m/s$ until the lateral acceleration reaches $1\,m/s^2$. The end

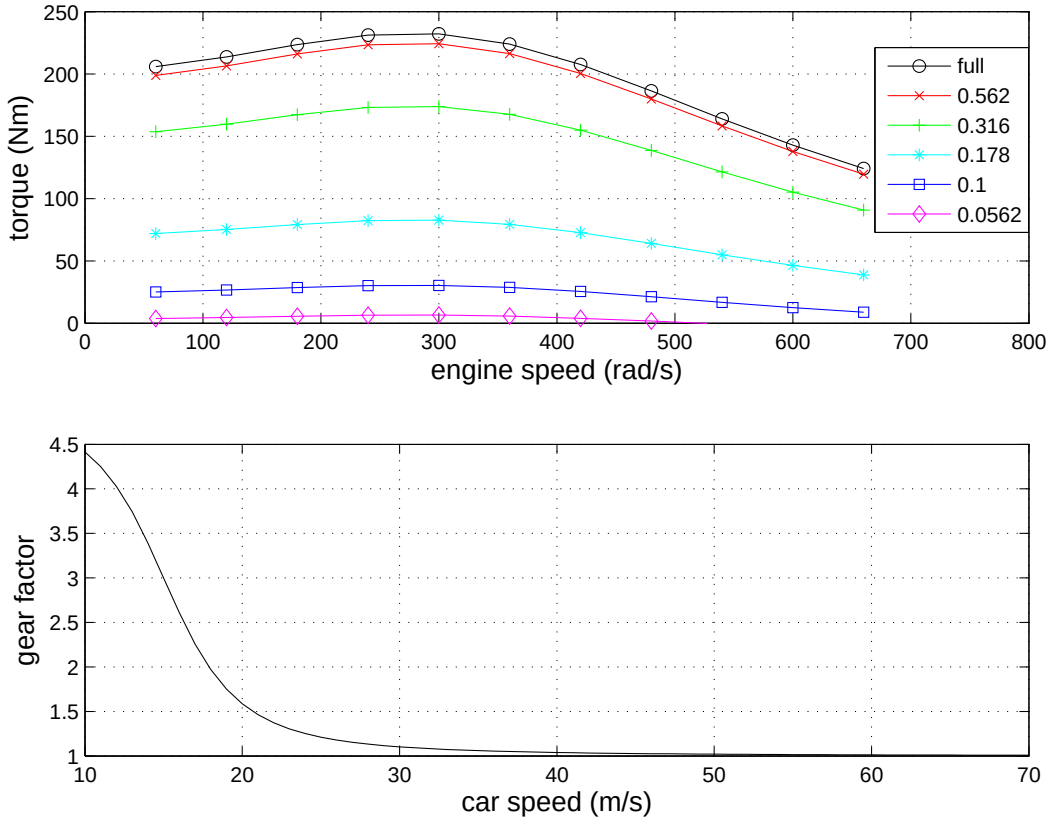

Figure 5. Engine torque as a function of engine speed and normalised throttle opening (upper) and gear ratio torque multiplier (lower).

condition is an approximate trim state, allowing rough optimal controls to be found for 10 m/s speed and 1 m/s^2 lateral acceleration. These controls are next used to track a circular path of radius 100 m at 10 m/s to establish a true trim state, for which an accurate optimal control set can be found. Repetition for lateral accelerations up to the possible limit in 1 m/s^2 steps and then for each of the other speeds allows the storage of a whole range of trim states and of the corresponding optimal controls. For speeds of 10, 20 and 30 m/s, a lateral acceleration of 10 m/s^2 could be sustained but for the higher speeds, 9 m/s^2 was the limiting value.

4.2 Optimal gains

Each optimal-gain set contains state-feedback and preview gains relating to each of the three controls allowed. The state-feedback gains are those of the standard Linear Quadratic Regulator problem [1, 2, 4, 6, 8] and are not so interesting. On the other hand, preview gains show some intriguing patterns that are worthy of illustration. Examples are given in Figures 6, 7 and 8 for an arbitrarily selected speed of 30 m/s. Similar figures relate to other speeds in the range. Figure 6 shows the gain sequences relating normalized throttle displacement to x-errors, Figure 7 shows those relating steering torque to x-errors and Figure 8 shows those relating steering torque to y-errors. The full set of gains includes throttle displacement to y-error and rider-upper-body lean torque to x-error and to y-error sequences, which are all relatively small and therefore not so significant. The symmetry of the straight-running case implies that cross-gains, relating throttle to y-errors or control

torque to x-errors should be zero for zero lateral acceleration, as indeed they are. However, as the lateral acceleration builds, so does the extent of the cross-coupling between the longitudinal control and the lateral errors and between the lateral controls and the longitudinal errors. The figures illustrate the full-preview idea, with each gain sequence converging on zero before the preview horizon is reached. For 30 m/s speed, the full 200 preview points are not, in fact, needed but they are for the highest speeds reachable. Figures 6 and 8 show the direct-gain sequences to follow patterns quite different from those of a car as the tyres approach saturation [10, 11], arising because the motorcycle tyres generate side-force primarily by cambering while those of a car do so by side-slipping.

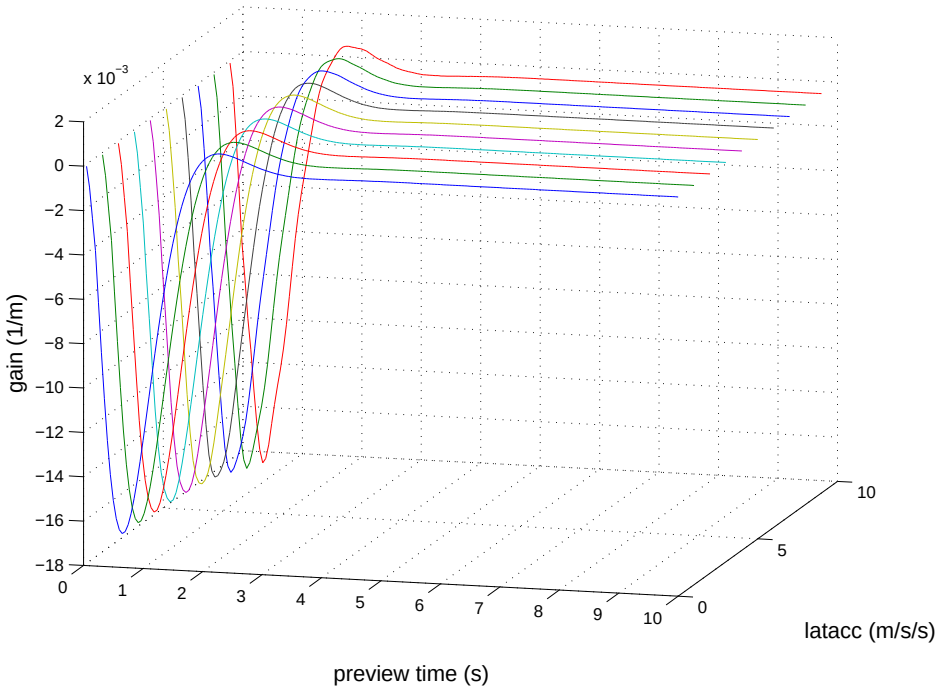

Figure 6. Optimal preview throttle displacement to x-error gain sequences as functions of lateral acceleration for 30 m/s speed and Ts=0.05 s.

4.3 Closed-loop system frequency responses

Each of the trim states stored has a corresponding optimal control. The control can be installed to the motorcycle to make a rider-controlled whole and the standard MATLAB function ”dbode” can be employed to compute the frequency responses of the closed-loop system. In each case, there are two situations to be treated, the one involving x-errors, the other, y-errors. In either event, the sinusoidal path perturbation implicit in frequency-response calculations is at the preview horizon and there is a transport delay associated with the travel of the motorcycle through the preview distance [4, 5, 9, 10, 11]. Perfect tracking is implied by a gain of unity or 0 dB and a system phase lag equal to the transport lag. Figures 9 and 10 demonstrate the tracking capabilities of an arbitrarily chosen system with 40 m/s speed and 6 m/s^2 lateral acceleration. The figures show that, for operation near to this trim state, perfect x-tracking will occur as long as the bandwidth of the disturbance is less than 0.7 rad/s and that perfect y-tracking will occur for bandwidths less than 0.5 rad/s. For frequencies higher than these limits, there will be some gain attenuation. Only

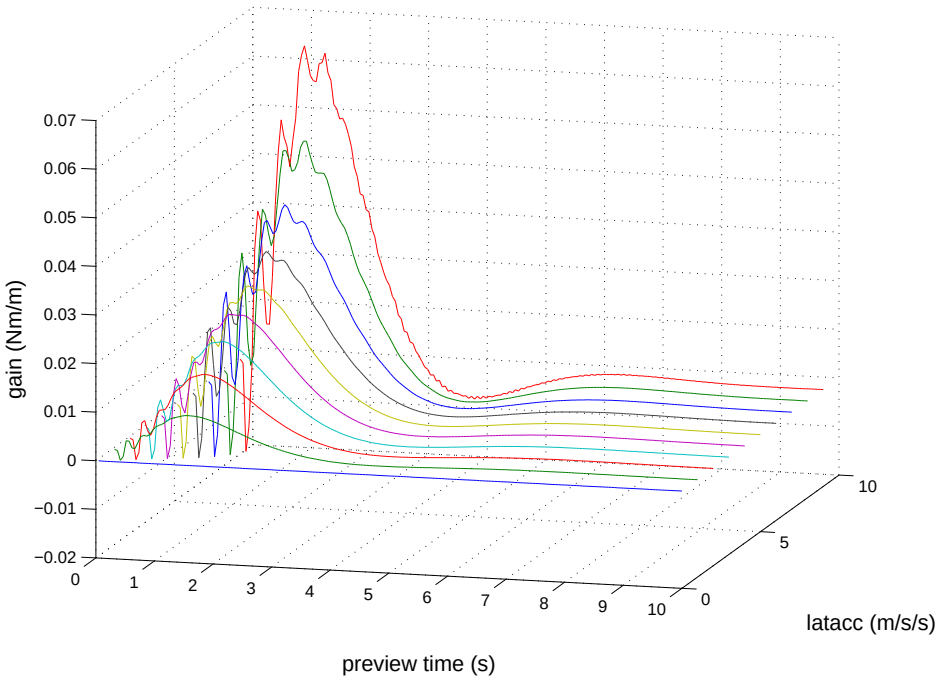

Figure 7. Optimal preview steer torque to x-error gain sequences as functions of lateral acceleration for 30 m/s speed and Ts=0.05 s.

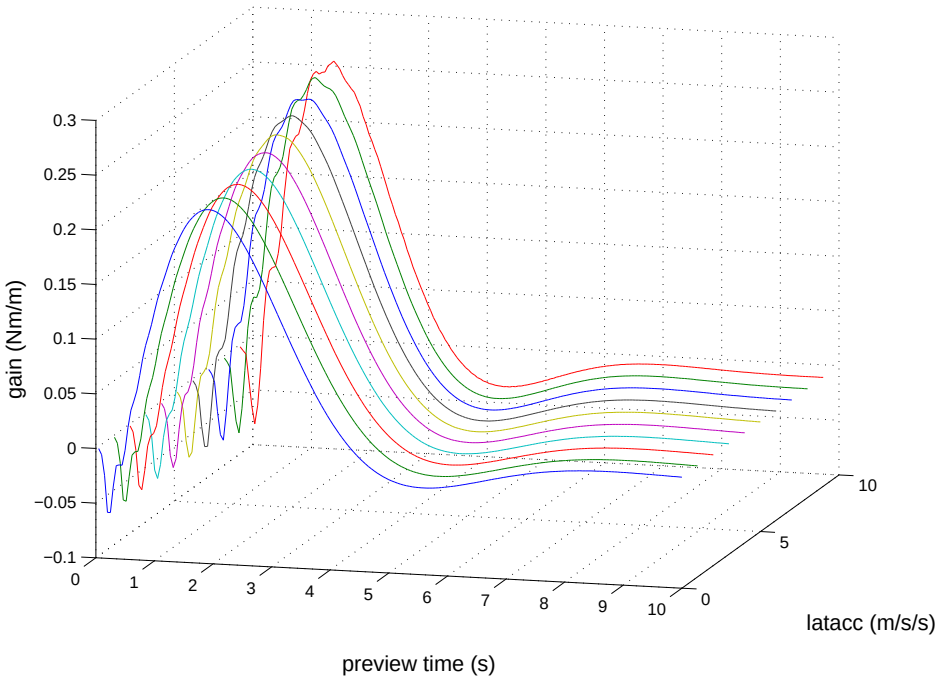

Figure 8. Optimal preview steer torque to y-error gain sequences as functions of lateral acceleration for 30 m/s speed and Ts=0.05 s.

for substantially higher-frequency disturbances will any significant phase distortion be introduced. The results shown are typical of those for other speeds and lateral accelerations.

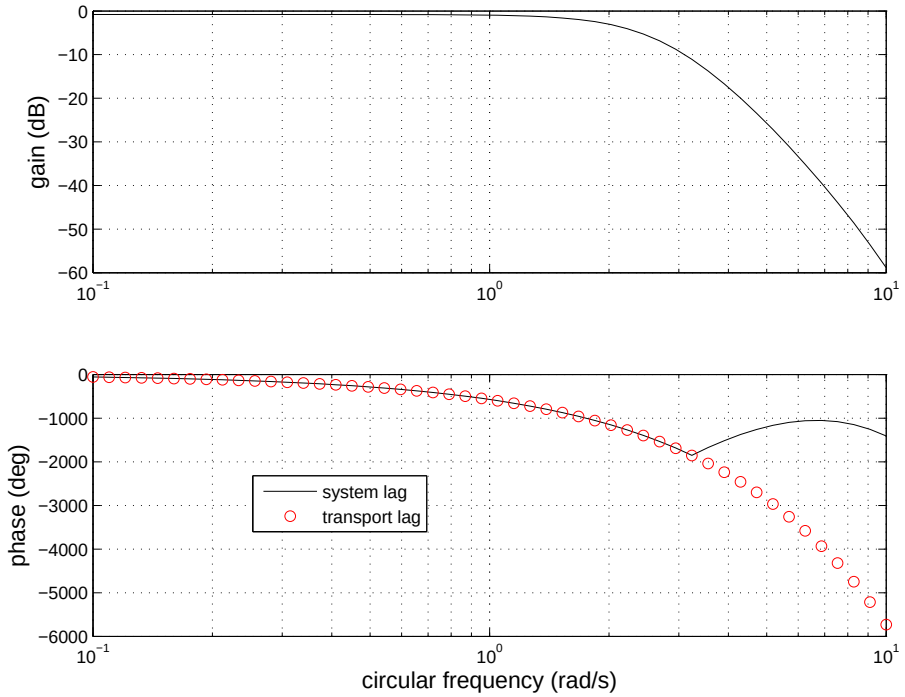

Figure 9. Closed-loop system frequency responses to x-perturbations for 40 m/s speed, 6 m/s^2 lateral acceleration trim state. x-tracking is almost perfect for frequencies less than 0.7 rad/s.

4.4 Path-tracking simulations

Tracking simulations are conducted under the following terms. Matrices of trim states, trim controls, state-feedback gains and preview gains, covering speeds of 10, 20, 30, ... 70 m/s and lateral accelerations of 0, 1, 2, ... 9 m/s^2 are supplied as data. The lateral symmetry of the motorcycle is exploited to avoid dealing with negative lateral accelerations. Initially, the rider-controlled machine is in a chosen trim state and the equations of motion of the closed-loop system are integrated using a 0.5 ms time step through 100 steps, updating the state by Ts, the discrete time step for the control calculations. For the next updating, the speed and lateral acceleration values are used in a bilinear interpolation scheme, (http://local.wasp.uwa.edu.au), to select the new trim states, trim controls and control gains. Integrations and adaptations follow in sequence, with storage of all the results needed for plotting, until the required number of simulation steps has been completed. Whenever the lateral acceleration is negative, the signs of the out-of-plane trim states and the steering and rider-lean torques are reversed.

To demonstrate the capacity of the control scheme to ensure good-quality tracking under near-limit running conditions, a path that starts with a straight, follows with a clothoid transition curve and then becomes circular is designed. The initial speed is taken as 10 m/s and the motorcycle is at trim for that speed and straight running. After a short time, a speed increase is demanded before the motorcycle reaches the transition curve. The speed increase demanded is tuned by trials so that the circular turn is traversed with extremely high lateral acceleration, actually reaching 10.76 m/s^2

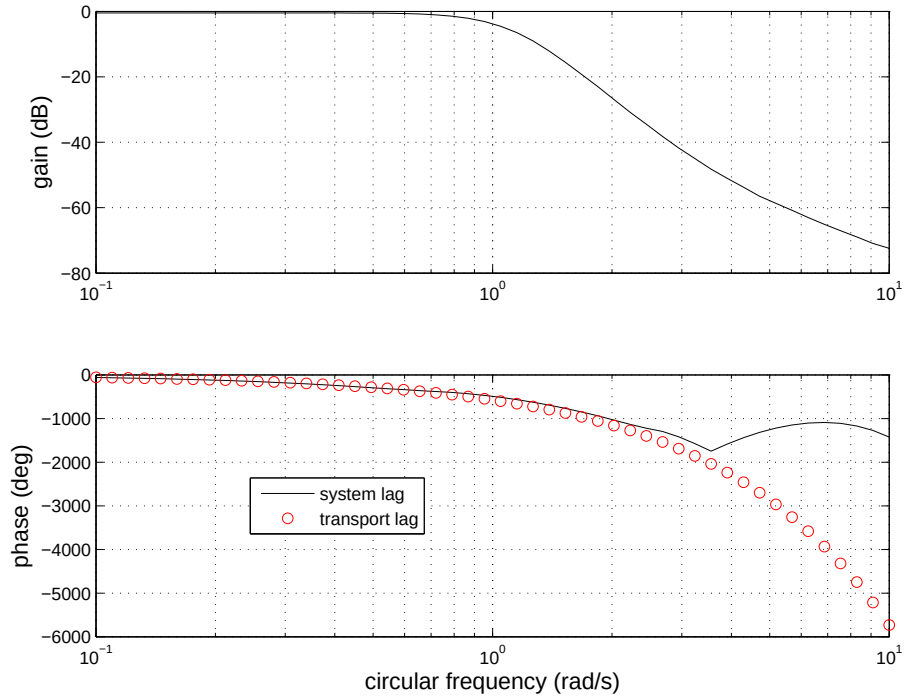

Figure 10. Closed-loop system frequency responses to y-perturbations for 40 m/s speed, 6 m/s^2 lateral acceleration trim state. y-tracking is almost perfect for frequencies less than 0.5 rad/s.

at one point in the run shown in Figures 11 and 12. In the first figure, the motorcycle path and the path demand are shown to be almost indistinguishable, the speed demand can be seen to be followed very closely and the throttle control input can be observed. In the second figure, rider lean torque and steer torque control inputs are plotted, the former being much smaller than the latter as in [3, 6, 7]. In the lower part, scaled angles include the swing arm angle, the steer angle, the rider-upper-body lean angle and the machine roll angle, which reaches $-54.5°$ just prior to the circular turn. The motorcycle pitch angle and the frame twist angle are not shown since they are rather small, varying between $-1.2°$ and $0.14°$ and between $-0.044°$ and $0.002°$ respectively.

Naturally, tracking runs result in failure if too much is demanded of the rider/machine combination. Paths are made difficult by sharp changes of direction which constitute higher-frequency excitation, see Figures 9 and 10, and, obviously, by high curvature and high speed. The looser the control is, that is the lower the values of the weights q_1 and q_2 used in the control computations, the more preview is required for full benefit but also the more smoothing of the path demand there is. Therefore, with loose control, it may not be so damaging to include sharp features in the path, but with tight control, rapidly varying control inputs will become necessary and this may lead to loss of control. Especially here, rapid steering is likely to excite the wobble mode into oscillation, the more so as the speed rises, since the damping of the mode becomes less as the speed rises from about 40 m/s [15]. Bursts of wobble-frequency control action can be seen in Figures 13 and 14 from a trial in which the path is a low-pass-filtered sinusoid following a straight, notwithstanding that the path and speed tracking are both excellent and the demand on the motorcycle is high. To eliminate that feature, the motorcycle or the controller or both would need further tuning. The machine at high speed would benefit from increased steering damping or the use of a steering

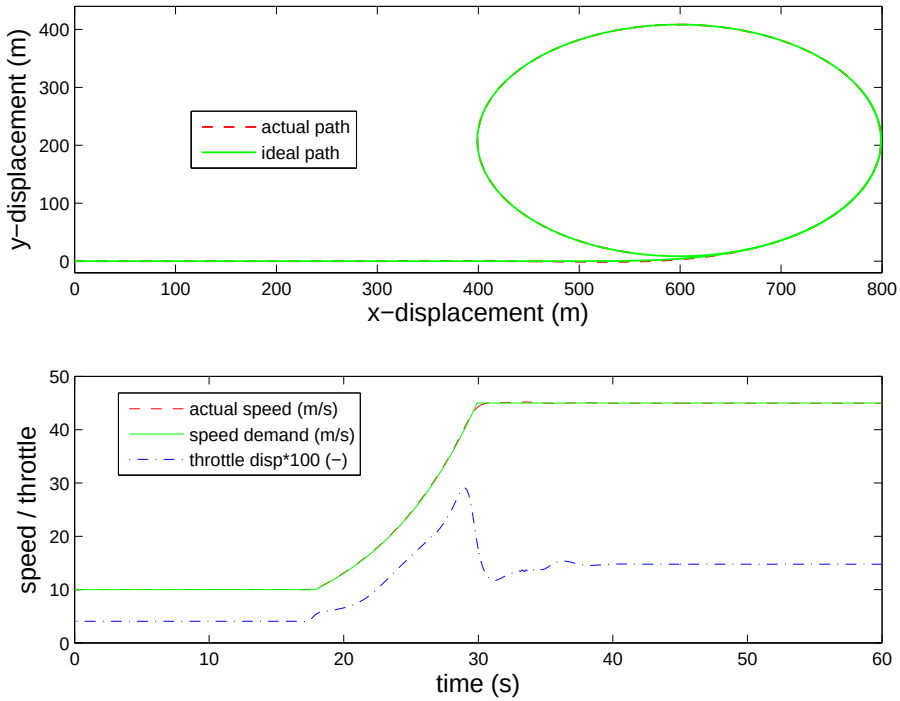

Figure 11. Path tracking of the rider-controlled motorcycle with bilinear adaptation of controls over speed and lateral acceleration. The path is shown in the upper part and the speed, speed demand and the normalized throttle displacement, the last scaled by a factor of 100, are shown in the lower part.

compensator [22, 23, 24, 25]. The rider would probably improve by the inclusion of bandwidth limitations to prevent unrealistically rapid control activity [12, 13, 14].

5 CONCLUSIONS

Accurate speed and steering control of a high-performance motorcycle near to its cornering limits have been shown to be possible using optimal linear quadratic regulator control methods with full preview of the path to be followed. Many trim states for variations in speed and lateral acceleration need to be found and the corresponding optimal controls determined off-line. Illustrative examples of the nature of the optimal preview gains as functions of time ahead, motorcycle speed and lateral acceleration have been included and the perfect tracking expected within the restrictions implied by small perturbations from a trim state have been demonstrated by closed-loop system frequency-response plots. In simulations, the trim states and the optimal controls constitute data and enable the identification by interpolation of trims and gains that provide a local reference for the motions, such that a linear treatment is appropriate. With the addition of special procedures for dealing with severe braking [26], it is likely that good tracking of general feasible paths will be possible even for racing conditions.

It is known from previous work that the closed-loop system bandwidth can be increased by using tighter control [4, 5, 9, 10, 11]. This is a mixed blessing, since loose control leads to path smoothing or corner cutting and this can contribute to robustness of the path-tracking performance. If

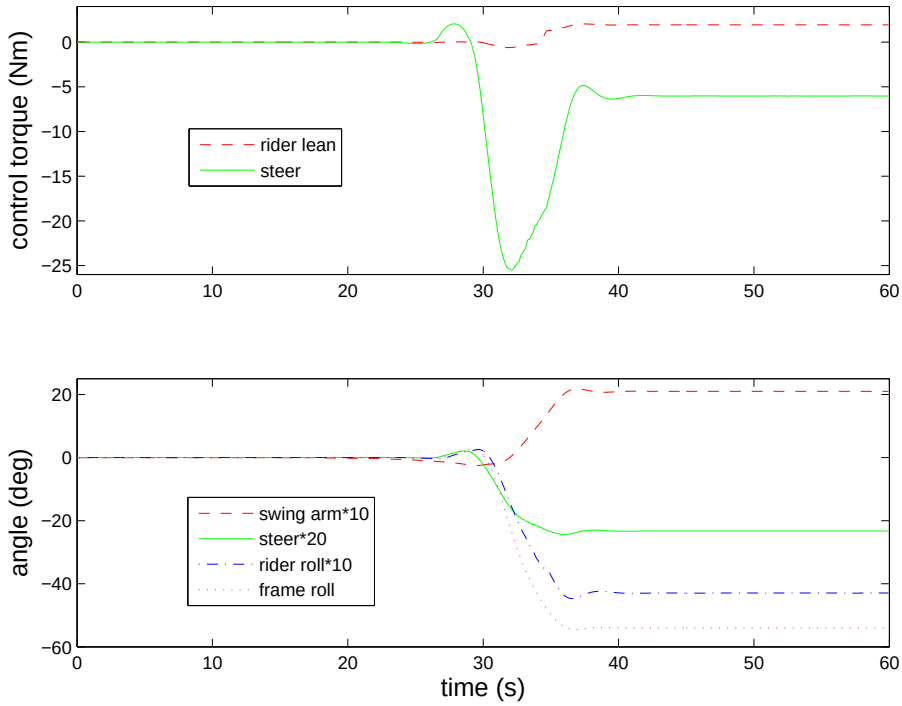

Figure 12. Path tracking of the rider-controlled motorcycle with bilinear adaptation of controls over speed and lateral acceleration. The upper part shows the rider lean and steer torque control inputs and the lower part shows scaled swing arm, steer, rider roll and frame roll angles.

the path to be followed is designed to be smooth in the first instance, this smoothing function will not be needed and it can be expected that tight control will be best. However, if the path contains sharp features implying higher-frequency disturbance to the motorcycle, looser control may well be better. In setting up a pilot with generally good properties, and in describing paths to be tracked, these are issues that need to be considered.

REFERENCES

[1] R. S. Sharp, and V. Valtetsiotis, ”Optimal preview car steering control”, ICTAM Selected Papers from 20th International Congress (P. Lugner and K. Hedrick eds), supplement to Vehicle System Dynamics 35, Swets and Zeitlinger (Lisse), 2001, 101–117.

[2] R. S. Sharp, ”Driver steering control and a new perspective on car handling qualities”, *Journal of Mechanical Engineering Science*, **219**(C8), 2005, 1041–1051.

[3] R. S. Sharp, ”Optimal linear time-invariant preview steering control for motorcycles”, The Dynamics of Vehicles on Roads and on Tracks (S. Bruni and G. Mastinu eds), supplement to Vehicle System Dynamics 44, Taylor and Francis (London), 2006, 329–340.

[4] R. S. Sharp, ”Optimal stabilisation and path-following controls for a bicycle”, *Proc. IMechE, Part C, Journal of Mechanical Engineering Science* **221**(C4), 2007, 415–428.

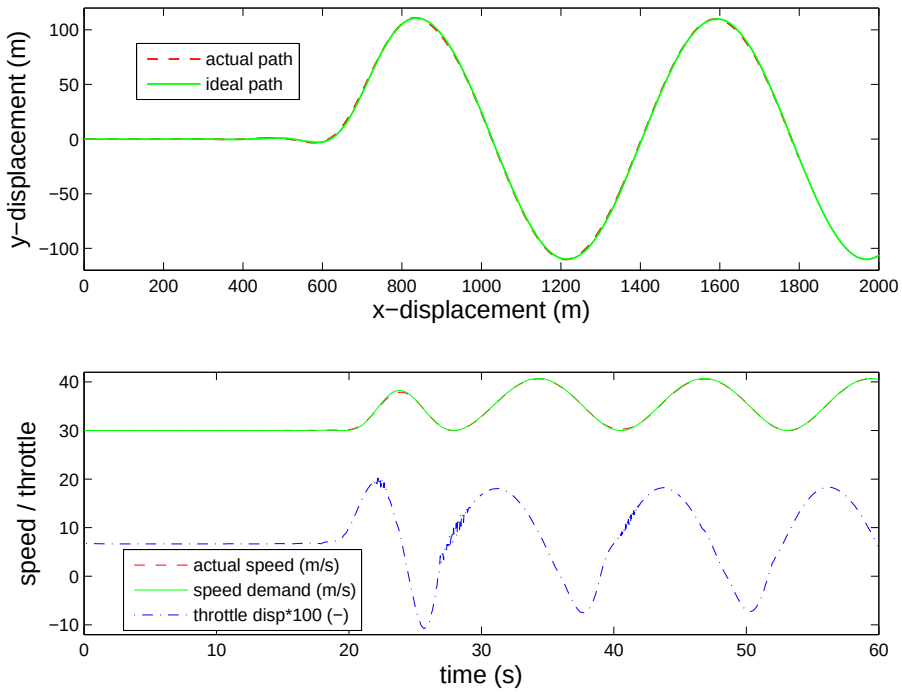

Figure 13. Path tracking of the rider-controlled motorcycle with bilinear adaptation of controls over speed and lateral acceleration. The path and speed demanded are followed with precision but short spells of unrealistic and unwanted throttle activity occur.

[5] R. S. Sharp, "Optimal preview speed-tracking control for motorcycles", in C. L. Bottasso, P. Masarati and L. Trainelli (eds), *Proc. Multibody Dynamics 2007, ECCOMAS Thematic Conference*, Milano, Italy, 25–28 June 2007, Politecnico di Milano, Milano, 16 pp.

[6] R. S. Sharp, "Motorcycle steering control by road preview", *Trans. ASME, Journal of Dynamic Systems, Measurement and Control* **129**(4), 2007, 373–381.

[7] R. S. Sharp, "Dynamics of Motorcycles: Stability and Control", in W. Schiehlen (ed.) *Dynamical Analysis of Vehicle Systems: Theoretical Foundations and Advanced Applications*, Springer, Wien/New York, 2007, 183–230.

[8] R. S. Sharp, "Optimal preview speed-tracking control for motorcycles", *Multibody System Dynamics* **18**(3), 2007, 397–411.

[9] R. S. Sharp, "On the stability and control of the bicycle", *Trans. ASME, Applied Mechanics Reviews* **61**, paper 060802, October 2008.

[10] M. Thommyppillai, S. Evangelou and R. S. Sharp, "Car driving at the limit by adaptive linear optimal preview control", *Vehicle System Dynamics*, **47**(12), 2009, 1535–1550.

[11] M. Thommyppillai, S. Evangelou and R. S. Sharp, "Rear-heavy car control by adaptive linear optimal preview", *Vehicle System Dynamics*, **48**(5), 2010, 645–658.

[12] R. S. Sharp, "On the stability and control of unicycles", *Proc. Roy. Soc., Series A*, published on-line 20/01/2010.

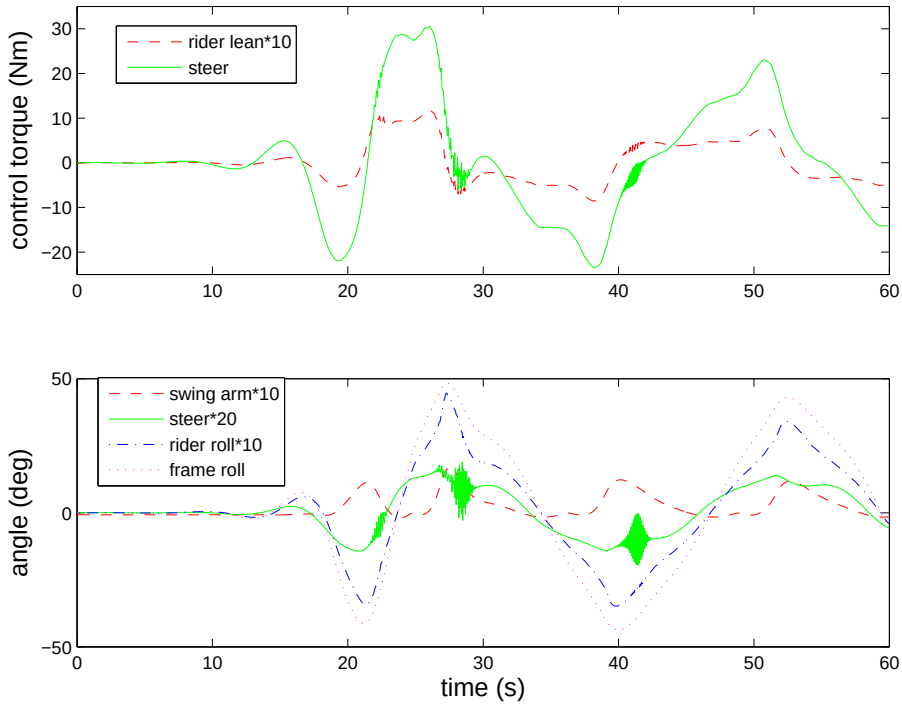

Figure 14. Path tracking of the rider-controlled motorcycle with bilinear adaptation of controls over speed and lateral acceleration. The upper part shows the rider lean and steer torque control inputs and the lower part shows scaled swing arm, steer, rider roll and frame roll angles. Short bursts of steering wobble oscillations are provoked by the controller on occasions.

[13] M. Thommyppillai, S. Evangelou and R. S. Sharp, "Advances in the development of a virtual car driver", *Multibody System Dynamics*, **22**(3), 2009, 245–267.

[14] M. Thommyppillai, S. Evangelou and R. S. Sharp, "Towards a practical virtual racing-car driver", *Proc. European Control Conference*, Budapest, Hungary, August 2009.

[15] R. S. Sharp, S. Evangelou and D. J. N. Limebeer, "Advances in the modelling of motorcycle dynamics", *Multibody System Dynamics*, **12**(3), 2004, 251–283.

[16] R. S. Sharp, S. Evangelou and D. J. N. Limebeer, "Multibody aspects of motorcycle modelling with special reference to Autosim", in J. G. Ambrï¿½sio (ed.), *Advances in Computational Multibody Systems*, Springer-Verlag, Dordrecht, The Netherlands, 2005, 45–68.

[17] B. D. O. Anderson and J. B. Moore, J. B, *Optimal Control: Linear Quadratic Methods*, Prentice Hall, Englewood Cliffs, NJ, 1989.

[18] A. Hazell, *Discrete-time optimal preview control*, PhD thesis, Imperial College London, 2008.

[19] S. Rowell, A. A. Popov and J. P. Meijaard, "Optimal control to modelling motorcycle rider steering: local versus global coordinate systems in rider preview", *Vehicle System Dynamics*, **48**(4), 2010, 429–456.

[20] A. A. Popov, S. Rowell and J. P. Meijaard, "A review on motorcycle and rider modelling for steering control", *Vehicle System Dynamics*, **48**(6), 2010, 775–792.

[21] I. N. Bronshtein and K. A. Semendyayev, *A Guide-Book to Mathematics*, Verlag Harri Deutsch, Frankfurt/Main and Zurich, 1971.

[22] S. Evangelou, D. J. N. Limebeer, R. S. Sharp and M. C. Smith, "Steering compensation for high-performance motorcycles", *Proc. 43rd IEEE Conference on Decision and Control*, Atlantis, December 2004, 749–754.

[23] S. Evangelou, D. J. N. Limebeer, R. S. Sharp and M. C. Smith, "Mechanical steering compensators for high-performance motorcycles", *Transactions of ASME, Journal of Applied Mechanics*, **69**(6), 2006, 724–739.

[24] S. Evangelou, D. J. N. Limebeer, R. S. Sharp and M. C. Smith, "Control of motorcycle steering instabilities: passive mechanical compensators incorporating inerters", *Proc. IEEE, Control Systems Magazine*, **26**(5), 2006, 78–88.

[25] S. Evangelou, D. J. N. Limebeer, R. S. Sharp and M. C. Smith, "An $\mathcal{H}_\infty$ loop-shaping approach to steering control for high-performance motorcycles", in Bruce A. Francis, Malcolm C. Smith and Jan. C. Willems (eds), *Control of Uncertain Systems: Modelling, Approximation, and Design*, Springer-Verlag, Berlin Heidelberg, 2006, 257–275.

[26] R. S. Sharp, "Application of Linear Optimal Preview Control Theory to Severe Braking of a Car", *Proc. IMechE, Part C, Journal of Mechanical Engineering Science*, accepted for publication 9/10/2010.